24th INTERNATIONAL CONGRESS ON SOUND AND VIBRATION
23–27 July 2017, London

# MACHINERY RADIATED NOISE EVALUATION OF UNDERWATER STRUCTURE WITH SPARSE SENSORS

Guo Cheng, Ruibiao Li, Lin He *and* Rongwu Xu
*Institute of Noise and Vibration, Wuhan, Hubei, China*
*email: s_t_unicorn@hotmail.com*

A radiated noise evaluation model of underwater structures is proposed, which is based on the operational transfer path analysis. The model can evaluate the main sinusoidal radiated noise of the structures with the sensors, which are fewer than sources of the structures. The model is turned into the traditional operational transfer path analysis out of the main sinusoidal signals. The lake experiment shows that, based on the proposed model, compared with the measuring results, the evaluating results of the main sinusoidal signals are less than 1.5dB; the trends of the wide bands are similar and the total error of the evaluation is less than 1dB.

Keywords: sparse sensors, radiated noise, sinusoidal signal, transfer path.

## 1. Introduction

Real-time evaluation of the underwater noise radiated by complex structures, is important in theoretical researches and engineering applications. At present, the methods of evaluation can be classified into two categories: calculation method which is based on the numerical models and experimental method which is based on the results of real tests. For the same requirement of accuracy, calculation method is more time-consuming and needs more sensors, so experimental method is dominantly adopted in practical applications[1-4].

A commonly used experimental method is the transfer path analysis (TPA), which can evaluate the radiated noise in real time based on the pre-measured transfer functions of different sound sources and the signals detected by the sensors mounted nearby the sources [5,6]. However, it is often difficult to obtain the transfer functions because actuation inside the structures or disassembly of device is required. Hence the model of operational transfer path analysis (OTPA) was proposed, which only requires to measure the response signals under varied operating modes before a structural-acoustic transfer matrix can be established if the principle of linear superposition is satisfied. Compared with the TPA method, the OTPA is simpler and suits for evaluating the noise radiated by complex structures [7-10].

Based on the traditional OTPA theory, however, the evaluated result of the radiated noise is not accurate, but a least square approximation. In many cases, the evaluated results are hard to be satisfied.

The exact radiated noise evaluation of the low frequency sinusoidal signals is a greater focus. A modified sinusoidal model of operational transfer path analysis is proposed in this paper, based on the evaluating requirement of the low frequency sinusoidal signals, and reduces the number of required sensors in the applications. Firstly, the theoretical basis of the model is founded. Secondly, simulation is conducted with reconstructed actuating signals and then the errors of the method are discussed. Thirdly, the model is validated in a lake experiment. Lastly, the conclusions of this study are drawn.

## 2. Basic Theory

### 2.1 Operational transfer path analysis

Assume that there are $S$ numbers of sources ($\mathbf{A}_S$), $R$ numbers of reference points ($\mathbf{X}_R$) and $O$ numbers of observation points ($\mathbf{Y}_O$) in a linear system. The influences of the sources on the

reference points and the observation points can be described with the transfer functions $\mathbf{H}^{r}_{S\times R}$ and $\mathbf{H}^{o}_{S\times O}$, so each response signal at the reference point can be expressed as:

$$\mathbf{X}_{M\times R}=\mathbf{A}_{M\times S}\mathbf{H}^{r}_{S\times R},\ \mathbf{Y}_{M\times O}=\mathbf{A}_{M\times S}\mathbf{H}^{o}_{S\times O} \tag{1}$$

where $M$ is the total number of different operating modes. Since the source signals cannot be measured directly, they are obtained with Eq.(1):

$$\mathbf{A}_{M\times S}=\mathbf{X}_{M\times R}\left(\mathbf{H}^{r}_{S\times R}\right)^{+} \tag{2}$$

From which we observe that, if $R<S$, the Eq. (2) is undetermined. Even though the transfer functions are invariant, only with the responses of the reference points, the characteristics of the sources are still hard to be uniquely determined. The responses of the observation points also cannot be uniquely determined with Eq. (1).

Combining Eq.(1) with Eq.(2) yields

$$\mathbf{Y}_{M\times O}=\mathbf{X}_{M\times R}\left(\mathbf{H}^{r}_{S\times R}\right)^{+}\mathbf{H}^{o}_{S\times O} \tag{3}$$

Let $\mathbf{T}_{R\times O}=\left(\mathbf{H}^{r}_{S\times R}\right)^{+}\mathbf{H}^{o}_{S\times O}$, and Eq.(3) can also be expressed as:

$$\mathbf{X}^{+}_{M\times R}\mathbf{Y}_{M\times O}=\mathbf{T}_{R\times O} \tag{4}$$

In this paper, $\mathbf{T}_{R\times O}$ is called transfer matrix. If $\mathbf{T}_{R\times O}$ can be determined via definite number of measurements, then the signals $\mathbf{Y}^{(1)}_{1\times O}$ at observation points under an arbitrary mode of operation can be evaluated as $\mathbf{Y}^{(2)}_{1\times O}$ in real time based on the signals at the reference points $\mathbf{X}'_{1\times R}$.

$$\mathbf{Y}^{(2)}_{1\times O}=\mathbf{X}'_{1\times R}\mathbf{T}_{R\times O} \tag{5}$$

Accordingly, the evaluated value $\mathbf{Y}^{(2)}_{1\times O}$ is equal to $\mathbf{Y}^{(1)}_{1\times O}$, only when $R\geq S$; and $\mathbf{Y}^{(2)}_{1\times O}$ is just a least square approximation under the condition of sparse sensors, when $R<S$.

## 2.2 Classification of the power in frequency domain

For the problem, future knowledge will be introduced. Most devices in underwater structures, such as pumps and shafts, are operating at one or more frequencies [11].

For a signal with frequency $f$, Eq.(2) can be expressed as

$$\mathbf{A}_{M\times S}(f)=\mathbf{X}_{M\times R}(f)\left(\mathbf{H}^{r}_{S\times R}(f)\right)^{+} \tag{6}$$

Although a large number of devices exist in an underwater structure, only a small number of devices generate significant noise with frequency $f$. The sinusoidal signals which are dominant in the some frequencies are called “characteristic sinusoidal signal”, and the frequencies are called “characteristic frequency”. According to the contributions of the sources, the power of the radiated noise is classified into three types:

power (1): the power of characteristic sinusoidal signals at the characteristic frequencies;

power (2): the power of the other signals at the characteristic frequencies;

power (3): the power at the other frequencies.

For example, there are three sources: source 1 includes characteristic sinusoidal signals F1 and F2 and white noise; source 2 includes characteristic sinusoidal signal G1 and white noise; source 3 only includes white noise. The focused spectrum of radiated noise is Z1~Z2.

The power of every source can be separated into four parts in frequency domain: the sinusoidal power at F1, the sinusoidal power at F2, the sinusoidal power at G1 and the other power in the band of Z1-Z2. So there are 3*4=12 parts in all.

According to the above classification, these parts can be classified as follows:

power (1): the power of source 1 at F1, the power of source 1 at F2, the power of source 2 at G1;

power (2): the power of source 1 at G1, the power of source 2 at F1, the power of source 2 at F2, the power of source 3 at F1, the power of source 3 at F2, the power of source 3 at G1;

power (3): the other power of source 1 in the band of Z1-Z2, the other power of source 2 in the band of Z1-Z2, the other power of source 3 in the band of Z1-Z2.

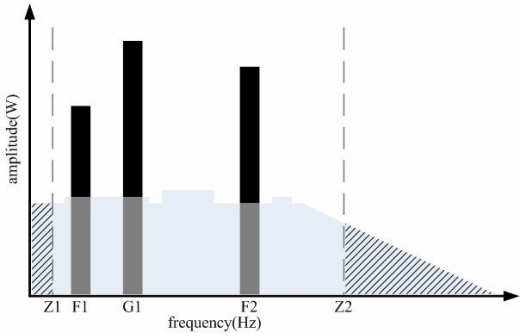


Figure 1 Power classification of the radiated noise
(power(1): blake; power(2): dark grey; power(3): french grey)

### 2.3 Evaluation of the sinusoidal power

The power (3) belongs to a large number of sources and the contribution of each one is insignificant. the evaluation theory of the power (3) is the same as traditional OTPA method.

The power (1) and the power (2) are at the same frequencies. The difference between them is that the power (2) can be ignored. Therefore, only the power (1) need to be considered. Assume that the number of the devices with the characteristic frequency $f$ is $N(f)$, and Eq.(6) becomes:

$$\mathbf{A}^{M\times N(f)}(f) \approx \mathbf{X}^{M}_{\times}{}^{R}(f)\left(\mathbf{H}^{N(f)\times R}(f)\right)^{+} \tag{7}$$

The number of the reference points is required to satisfy "$R \geq N_{\max}(f)$", where $N_{\max}(f)$ is the maximum of $N(f)$ for all characteristics frequencies $f$. In this case, Eq.(7) is not only the optimal approximation under the sparse-sensor condition, but also the exact solution at some characteristic frequencies.

### 2.4 Control of the evaluation error

Based on the above theory, the evaluated value of the power (1) is exact. Compared with the power (1), the power (2) can be ignored. However, the evaluated value of the power (3) is a least square approximation, and it is the primary source of the error.

The key to control the evaluation error of the power (3), is the reduction of the approximation error.

$$\mathbf{Y}^{(2)}_{1\times O} = \mathbf{X}'_{1\times R}\left(\mathbf{H}^{r}_{S\times R}\right)^{+}\mathbf{H}^{o}_{S\times O} \tag{8}$$

Where $R < S$. According to the definition of the Moore-Penrose inverse and the theory of the least square approximation, the evaluated value is the result of the minimum standard deviation. The operating mode which is used to generate the transfer matrix is called "training mode". So if the gap between the radiated noise of the evaluated mode $\mathbf{Y}^{(1)}_{1\times O}$ and the radiated noise of the training mode $\mathbf{Y}_{M\times O}$ is smaller, the evaluated result will be exacter.

In real evaluation, the radiated noise of the evaluated mode $\mathbf{Y}^{(1)}_{1\times O}$ is unknown. The training modes can be selected based on the responses of the reference points and the settings of the modes.

## 3. Numerical simulations

### 3.1 Problem statement and simulation procedure

Based on the noise signals of real devices, the simulation data is constructed. For the convenience of discussion, assume that there are 3 devices in a structure. The actuating signals caused by these devices are composed of the background noise, white noise (1-1600Hz), low-frequency wide-band noise (300-1000Hz) and stochastic sinusoidal signals. Fig. 2 shows the radiated noise signal when a device operates solely.

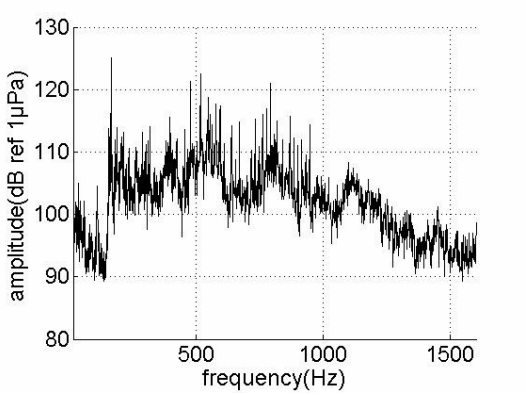


Figure 2 The radiated sound pressure signal of a simulated device

Two well separated reference points are selected at the center of the structure, and two accelerometers are mounted there to record the vibration responses under internal actuation. A hydrophone array is placed 25 m away from the structure for recording the average sound pressure radiation under the excitation of devices inside the structure. For the convenience of discussion, the sampling frequency is set as 4096Hz for the signals collected by both hydrophones.

The operating modes generated in the simulation are shown in Table 1.

Table 1: The simulated devices in different operating modes.

| mode | device1# | device2# | device3# |
|---|---|---|---|
| 1 | % | % | % |
| 2 | % | | |
| 3 | | % | |
| 4 | | | % |
| 5 | % | % | |
| 6 | | % | % |
| 7 | % | | % |

The vibration data at reference points and the radiated noise in the combination of different operating modes are obtained by superposition of the data when the devices operate individually. In the table, the symbol “%” means that the device is operating.

### 3.2 Simulation result

The validity of the proposed model is verified first. The operating modes 2 to 4 are defined as training modes, and the operating mode 1 are defined as evaluated mode. The transfer matrix is derived with the data of the operating modes from No.2 to No.4. The radiated noise in the No.1 operating mode is then evaluated based on the derived transfer matrix and the vibration data at the reference points in the No.1 operating mode.

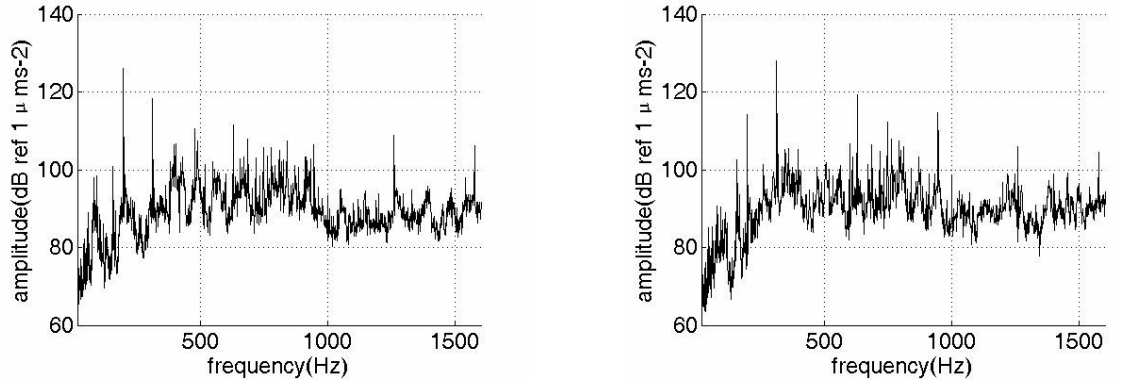


A. At reference point 1 B. At reference point 2

Figure 3 Vibration data of the No.1 operating mode

As shown in Fig.4, the primary characteristic sinusoidal signals of the operating mode 1 radiated noise are: 46Hz, 168Hz, 200Hz, 315Hz, 400Hz, 480Hz.

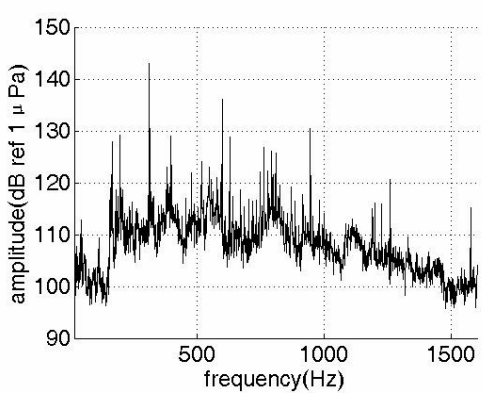


Figure 4 Radiated noise of the No.1 operating mode

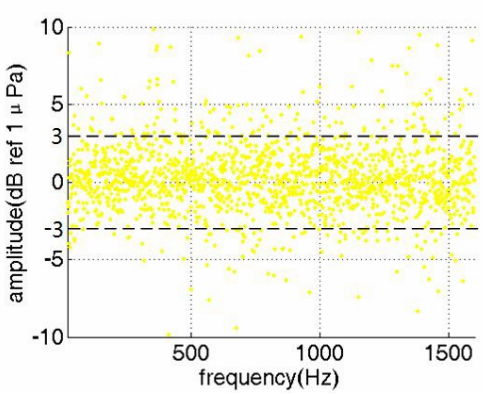


Figure 5 The evaluated error of the radiated sound pressure in the simulation (training mode: mode 2 to 4)

Figure 5 shows that at most frequency points, including the most characteristic frequency points shown in Fig.4, the errors are less than 3dB. Only at minor part of the frequency points, the errors are large. The average error of the wide band is less than 2dB and the errors of the mainly characteristic sinusoidal signals are as follows:

| Frequency(Hz) | 46 | 168 | 200 | 315 | 400 | 480 |
|---|---|---|---|---|---|---|
| Error(dB) | 4.244 | 0.026 | 0.0275 | 0.020 | 0.295 | 0.483 |

Then validate the influence of the training-mode selection on the evaluating error. The operating modes from No.5 to No.7 are defined as training modes. The noise radiated in the No.1 operating mode is also evaluated.

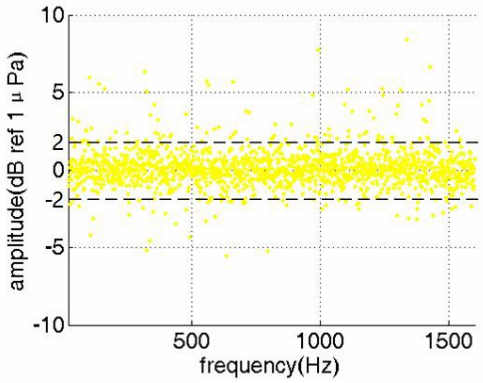


Figure 6 The evaluated error of the radiated sound pressure in the simulation (training mode: mode 5 to 7)

As the results shown in Fig.6, The noise radiation in the No.1 operating mode evaluated with the No.5 to No.7 operating modes is more accurate. The errors at most frequencies are less than 2dB in the sound pressure spectrum, In wide band, the error is less than 1dB, which is smaller than the errors of the former evaluation results based on the data of the operating modes from No.2 to No.4. The errors of the mainly characteristic sinusoidal signals are as follows:

| Frequency(Hz) | 46 | 168 | 200 | 315 | 400 | 480 |
|---|---|---|---|---|---|---|
| Error(dB) | 1.797 | 0.060 | 0.0895 | 0.006 | 0.112 | 0.249 |

Because the No.5-7 operating modes are more similar to the No.1 mode, compared with the No.2-4 operating modes, better wide-band evaluation results are obtained with the selection of the No. 5-7 training modes. For characteristic sinusoidal signals, the gap is negligible. Therefore, to reduce the wide-band error of noise evaluation in engineering applications, the training modes can be classified first before further calculation.

# 4. Experimental validations

## 4.1 Experimental setup and procedure

The proposed model is also validated by experiments conducted in the Thousand Islands Lake. The experiment site is located in an inlet, and the water waves and background noise in the inlet is negligible.

The tested structure is a 2.05-m-long cylinder with double-layer shell. The outer shell has 1.78 m diameter, and is 2 mm thick; the diameter of its inner shell is 1.46m, and the thickness is 8mm. The shell is supported by four equally spaced annular plates. The shell is airtight with 25-mm-thick stainless steel plates at both ends, and water is filled in the space between the inner and outer shells. In the interior of the inner shell, an 8-mm thick plate is fixed, on which a small air compressor (whose inlet and outlet valves are both open) and an actuator are mounted. A reference accelerometer is also mounted inside the shell, and a power cable and two signal cables come out of the cylinder through three holes on an end plate.

The cylinder shell is suspended underwater by a crane on the bank. Four hydrophones are fixed to a boat anchored in 5.7-m distance away from the shell.

Figure 7 The environment and model of the experiment

The following procedure is designed and implemented in the experiments:

(1) Suspend the cylinder shell underwater, start the air compressor, and record and analyze the acceleration signal recorded by the accelerometer on the shell and the radiated sound pressure at the location of the boat.

(2) Keep the air compressor to operate and activate the actuator in the shell using powered signal with sinusoidal signals superposed by white noise. Record and analyze the signals listed in step (1).

(3) Stop the air compressor, and only activate the actuator. Record and analyze the signals as at step (2).

## 4.2 Experimental results

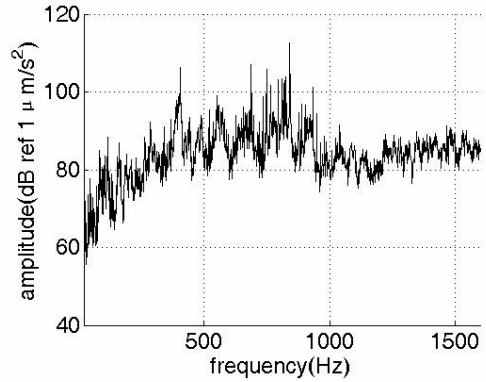


a. the response signal of the acceleration at the reference point

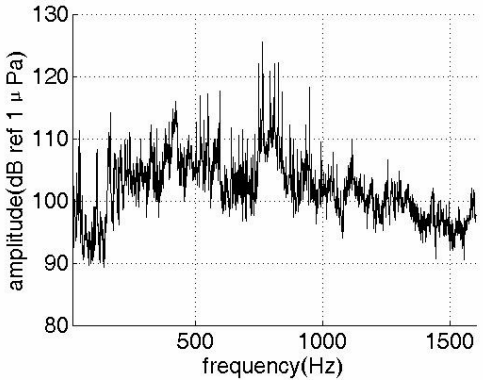


b. the sound pressure signal of the radiated noise

Figure 8 The signals of the air compressor

For the limit of experimental condition, only the radiated noise evaluation of two devices with one acceleration is validated. Without loss of generality, the transfer matrix is generated with the data acquired at step (1) and (3), and the radiated noise at step (2) is evaluated.

Figure 8 shows the acceleration signal at the reference point and the radiated noise signal when the air compressor is operating solely. The level of vibration is about 60-110dB, and the level of the radiated noise is about 90-125dB.

Figure 9 shows the acceleration signal at the reference point and the radiated noise signal for step (3) when the actuator is operating solely. The characteristic frequencies of the actuator are widely distributed in the entire analysis frequency range. The level of vibration is about 50-110dB, and the level of radiated noise is about 80-130dB; both are equivalent to the actuating intensity of the air compressor.

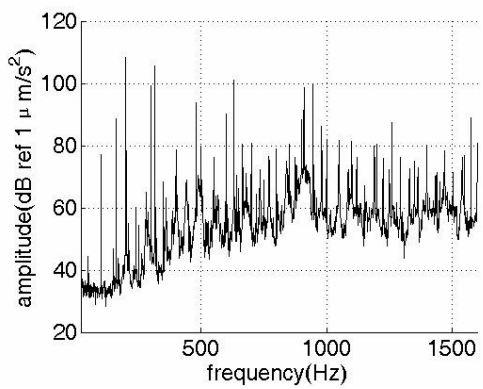


a. the response signal of the acceleration at the reference point

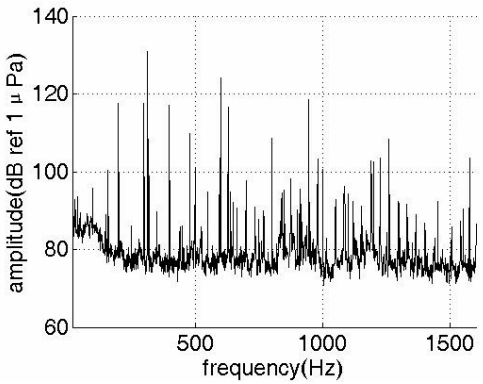


b. the sound pressure signal of the radiated noise

Figure 9 The signals of the actuator

Based on the transfer matrix derived with the data obtained at step (1) and (3), and along with the acceleration signal at the reference point of step (2), the noise radiated at step (2) is evaluated.

As shown in Fig.10, the primary characteristic sinusoidal signals of radiated noise include: 23Hz, 38Hz, 46-49Hz, 103Hz, 160Hz, 168Hz, 200Hz, 250Hz, 315Hz.

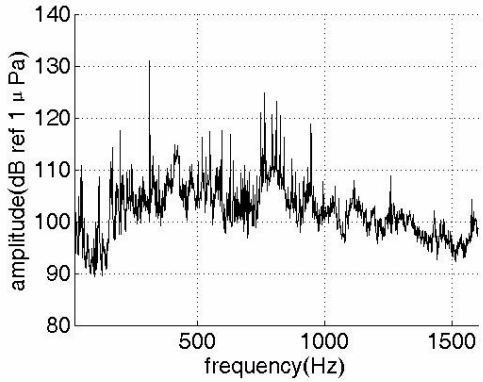


Figure 10 Radiated noise of the step (2)

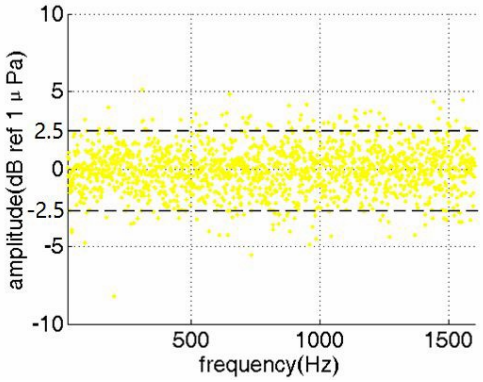


Figure 11 The evaluated error of the radiated sound pressure

The gap between the evaluated and the measured sound pressure is shown in Fig.11. The errors are less than 2.5dB at most frequencies, and the error of the wide band is less than 1dB. The errors of the characteristic sinusoidal signals are as follow. Most of them are less 1.5dB:

| Frequency(Hz) | 23 | 38 | 46-49 | 103 | 160 | 168 | 200 | 250 | 315 |
|---|---|---|---|---|---|---|---|---|---|
| Error（dB） | 0.425 | 0.172 | 0.210 | 1.096 | 0.513 | 0.445 | 8.184 | 1.128 | 3.141 |

## 5. Conclusion

For the real-time evaluation of the underwater structure radiated noise, based on the operational transfer path analysis with sinusoidal signals, a modified sinusoidal evaluation model is proposed. Numerical verification and experimental validation of the proposed model show that:

(1) The proposed sinusoidal evaluation model is effective, and the number of sensors is reduced in the evaluation of the radiated noise.

(2) The selection of the training modes which are closer to the evaluated mode, would help to improve the wide-band evaluating accuracy.

(3) In the lake experiment, the error of the wide band is less than 1dB, and the errors at most characteristic sinusoidal signals are less than 1.5dB.

## REFERENCES


1 Wu Xian-Jun, Lv Ya-dong, Sui Fu-sheng. A perfect OPAX method for vibration transfer path analysis combined with OTPA method[C]. *The 22nd international congress on sound and vibration,* Florence, Italy: 1-8, (2015).

2 A.T. Moorhouse, A. S. Elliott, T. A. Evans. In Situ Measurement of the Blocked Force of Structure-borne Sound Sources[J]. *Journal of Sound and Vibration*, **325**: 679-685, (2009).

3 Jorge P. Arenas. Numerical computation of the sound radiation from a planar baffled vibrating surface[J]. *Journal of Computational Acoustics,* **16**(3): 321-341, (2008).

4 X. Zhu, T.Y. Li, Y. Zhao, J. Yan. Vibrational power flow analysis of thin cylindrical shell with a circumferential surface crack[J]. *Journal of Sound and Vibration,* **302**: 332–349, (2007).

5 A.S.Elliott, A.T.Moorhouse, T.Huntley, S.Tate. In-situ source path contribution analysis of structure borne road noise[J]. *Journal of Sound and Vibration,* **332**: 6276–6295, (2013).

6 ZHANG Lei, CAO Yue-yun, YANG Zi-chun, HE Yuan-an. Vibration-acoustic transfer path analysis of a submerged cylindrical double-shell[J]. *Journal of Ship Mechanics,* **19**(4): 462-469, (2015).

7 D. deKlerk, A.Ossipov. Operational transfer path analysis: Theory, guidelines and tire noise application[J]. *Mechanical Systems and Signal Processing,* **24**: 1950–1962, (2010).

8 C.Sandiera, Q.Leclerea, N.B.Roozen. Operational transfer path analysis: theoretical aspects and experimental validation[C]. *ACOUSTICS,* (2012).

9 Alex Sievi, Frank Steinbach. Operational transfer path analysis for validation of the prediction models for high-speed trains[C]. *The 21st international congress on sound and vibration,* Beijing, China: 1-8, (2014).

10 N.B. Roozen, Q. Leclere, C. Sandier. Operational transfer path analysis applied to a small gearbox test set-up[C]. *ACOUSTICS,* (2012).

11 Yan Li, Lin He, Chang-geng Shuai, Fei Wang. Time-domain filtered-x-Newton narrowband algorithms for active isolation of frequency-fluctuating vibration [J]. *Journal of Sound and Vibration,* **367**, (2016).